Entanglement properties of topological color codes

Mehdi Kargarian*
Physics Department, Sharif University of Technology, Tehran 11155-9161, Iran
(Received 29 September 2008; published 5 December 2008)

The entanglement properties of a class of topological stabilizer states, the so-called *topological color codes* defined on a two-dimensional lattice or *2-colex*, are calculated. The topological entropy is used to measure the entanglement of different bipartitions of the 2-colex. The dependency of the ground-state degeneracy on the genus of the surface shows that the color code can support a topological order, and the contribution of the color in its structure makes it interesting to compare with Kitaev's toric code. While a qubit is maximally entangled with the rest of the system, two qubits are no longer entangled showing that the color code is genuinely multipartite entangled. For a convex region, it is found that entanglement entropy depends only on the degrees of freedom living on the boundary of two subsystems. The boundary scaling of entropy is supplemented with a topological subleading term, which for a color code defined on a compact surface, is twice over the toric code. From the entanglement entropy we construct a set of bipartitions in which the diverging term arising from the boundary term is washed out, and the remaining nonvanishing term will have a topological nature. Besides the color code on the compact surface, we also analyze the entanglement properties of a version of color code with a border, i.e., *triangular color code*.

DOI: 10.1103/PhysRevA.78.062312 PACS number(s): 03.67.Lx, 03.67.Mn, 03.65.Ud, 42.50.Dv

I. INTRODUCTION

In quantum information theory and quantum computations, entanglement is recognized as an essential resource for quantum processing and quantum communications, and it is believed that the protocols based on the entangled states have an exponential speedup over the classical ones. Besides, in highly correlated states in condensed-matter systems such as superconductors [1,2] and fractional quantum Hall liquids [3], the entanglement serves as a unique measure of quantum correlations between degrees of freedom. In quantum many-body systems such as spin, fermion, and boson systems, the entanglement is connected to the phase diagram of the physical systems. Nonanalytic behavior of entanglement close to the quantum critical point of the system and the occurrence of finite-size scaling have provided intense research leading us to refresh our insight of the critical properties from the quantum information side. For a comprehensive discussion, see the review by Amico *et al.* [4], and references therein. In recent years the appearance of new phases of matter has intensified the investigation of entanglement in quantum systems. These are phases beyond the Landau-Ginzburg-Wilson paradigm [5], where an appropriate local order parameter characterizes different behaviors of two phases on either side of the critical point. These new phases of matter carry a kind of quantum order called *topological order* [6] and the transition among various phases does not depend on the symmetry-breaking mechanism. Therefore the Landau theory of classical phase transition fails in order to describe these phases. The ground state of such phases is a highly entangled state and the excitations above the ground state have a topological nature, which is mirrored in their exotic statistics.

Among the models with topological properties, the Kitaev or toric code [7] has been extensively studied. Ground-state degeneracy depends on the genus or handles of the manifold that the model is defined on, and there is a gap that separates the ground-state subspace from the excited states. The ground-state degeneracy cannot be lifted by any local perturbations, which underlines Kitaev's model as a test ground for fault-tolerant quantum computations [7]. The ground state of Kitaev's model is indeed stabilized by the group generated by a set of local operators called *plaquette* and *star* operators, making it useful as a quantum error-correcting code [8]. The information is encoded in the ground-state subspace, which is topologically protected making it robust as a quantum memory [9]. For this model any bipartition of the lattice has nonzero entanglement, which manifests the ground state is generically multipartite entangled [10]. Bipartite entanglement scales with the boundary of the subsystem, showing that the entanglement between two parts of the system depend only on the degrees of freedom living on the boundary, which is a manifestation of the holographic character of the entanglement entropy [11].

For topological models a satisfactory connection between topological order and entanglement content of a model has been established via introducing the concept of the *topological entanglement entropy* (TEE) [12,13] which is a universal quantity with topological nature.

Another resource with topological protection character is called *color code*. An interplay between color and homology provides some essential features; for example, a particular class of two-dimensional color codes with colored borders will suppress the need for selective addressing to qubits through the implementation of the Clifford group [14]. The number of logical qubits that are encoded by a two-dimensional color code are twice over the toric code [15] defined on the compact surface.

In this paper we study the entanglement properties of a color code defined on a two-dimensional lattice, the so-called 2-colex [16]. We consider different bipartitions of the lattice and evaluate the entanglement entropy between them. The

*kargarian@physics.sharif.edu

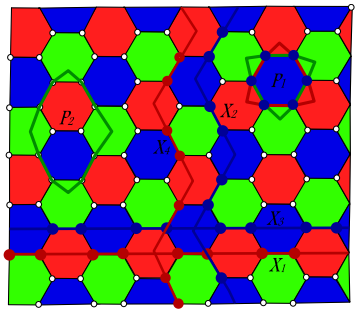

FIG. 1. (Color online) A piece of 2-colex, which has been defined on the hexagonal lattice with periodic boundary conditions. Lightest to darkest hexagons: green, red, and blue, respectively. All circles stand for qubits living at the vertices. A hexagon (P_1), say blue, can be denoted by either a red or green closed boundary string, and the product of two neighboring plaquettes, say red and blue, corresponds to a green string (P_2). Noncontractible loops (X_1, X_2, X_3, X_4) stand for topological color codes, which determine the structure of the encoded subspace $\mathcal{C}$. A colored string connects plaquettes with the same color.

connection between the topological nature of the code and the entanglement entropy is also discussed.

The structure of the paper is as follows. In Sec. II the basic notions of a color code on the surface is introduced. In Sec. III, based on the stabilizer structure of the protected code space, the reduced density matrix, which is needed for evaluating the entanglement entropy, is calculated. Then in Sec. IV the entanglement entropy for different bipartitions is calculated. In Sec. V another class of color code on plane and its entanglement properties are introduced, and the finally, Sec. VI is devoted to the conclusions.

II. PRELIMINARIES ON TOPOLOGICAL COLOR CODE

In this paper we consider a class of topological quantum error-correction code defined on the lattice, the so-called topological color codes (TCC) [14]. The local degrees of freedom are spin-1/2 with the bases of the Hilbert space C^2. The lattice we consider is composed of vertices, links, and plaquettes. Each vertex stands for a local spin. Three links meet each other at a vertex and no two plaquettes with the same color share the same link. We suppose this color structure is denoted by the notation TCC$\{V,E,P\}$ where V,E,P denotes the set of vertices, edges, and plaquettes, respectively. For simplicity we define the model on the regular hexagonal lattice on the torus, i.e., imposing periodic boundary conditions as shown in Fig. 1. There is a subspace $\mathcal{C}\subset\mathcal{H}$, which is topologically protected. The full structure of this subspace and its properties are determined by a definition of the stabilizer group. The stabilizer group is generated by a set of plaquette operators. For each plaquette we attach the following operators, which are products of a set of Pauli operators of vertices around a plaquette:

$$\Omega_p^C = \bigotimes_{v\in p} \Omega_v^C, \quad \Omega = X,Z, \quad C = \text{red, green, blue}. \tag{1}$$

For a generic plaquette, say blue plaquette P_1 in Fig. 1, we can identify green and red strings, which are the boundary of the plaquette. It is natural to think of the product of different plaquette operators, which may produce a collection of boundary operators. For example, as is shown in Fig. 1, the product of two neighboring plaquettes, say red and blue ones, correspond to a green string P_2, which is a boundary of two plaquettes. All string operators produced in this way are closed. Since all closed strings share either nothing or an even number of vertices, they commute with each other and with plaquettes. In addition to closed boundary operators, there are other closed strings, which are no longer the product of the plaquette operators. These closed strings form the fundamental cycles of the manifold in which the lattice is defined on and have a character of color. The number of these closed loops depends on the genus of the manifold in which the lattice is defined on. For the torus with $g=1$ there are two such cycles that are noncontractible loops in contrary to the closed boundary strings, which are homotopic to the boundary of a plaquette. For the topological color codes these noncontractible loops are shown in Fig. 1. For every homology class of the torus there are two closed strings, each of one color, say red and blue. The red string connects red plaquettes and so on. Note that a generic string, say green, can be produced by the product of the red and blue strings when they are suitably chosen. In fact, since every Pauli matrix squares identity, at a vertex (qubit) where two homologous strings cross each other, they cancel each other. Indeed there is an interplay between color and the homology class of the model. One can define a nontrivial closed string as follows:

$$\mathcal{S}_\mu^{C\Omega} = \bigotimes_{i\in I} \Omega_i, \tag{2}$$

where I indexed the set of spins on a generic string, μ stands for the homology class of the torus, and Ω is the X or Z Pauli spin operators. Closed noncontractible loops turn on to form bases for the encoded logical operators of topological code. To clarify this, we label different loops as

$$X_1 \leftrightarrow \mathcal{S}_2^{RX}, \quad X_2 \leftrightarrow \mathcal{S}_1^{BX}, \quad X_3 \leftrightarrow \mathcal{S}_2^{BX}, \quad X_4 \leftrightarrow \mathcal{S}_1^{RX},$$

$$Z_1 \leftrightarrow \mathcal{S}_1^{BZ}, \quad Z_2 \leftrightarrow \mathcal{S}_2^{RZ}, \quad Z_3 \leftrightarrow \mathcal{S}_1^{RZ}, \quad Z_4 \leftrightarrow \mathcal{S}_2^{BZ}. \tag{3}$$

These operators form a four-qubit algebra in $\mathcal{H}_2^4$, so it manifests a 16-dimensional subspace for the coding space $\mathcal{C}$, which is topologically protected. On the other hand, the topological color code on the torus with $g=1$ encodes four qubits. Now we move to construct the explicit form of the states of the subspace $\mathcal{C}$.

The above construction for the string operators in Eq. (3) can be extended to an arbitrary manifold with genus g. For such a manifold the coding space is panned with 2^{4g} vectors. Note that for the toric code (white and dark code) [15] when it is embedded in the same manifold with genus g, the coding space will span with 2^{2g} vectors [10], which explicitly shows that the color codes have a richer structure than the toric codes [15].

A. Stabilizer formalism

The protected subspace $\mathcal{C}$ is spanned by the state vectors, which are stabilized by all elements of the stabilizer group,

i.e., a subset of the Pauli group. Let $\mathcal{U}$ be a set of generators of the stabilizer group and its elements are denoted by $\mathcal{M}$. So this subspace is

$$\mathcal{C} = \{|\psi\rangle: \mathcal{M}|\psi\rangle = |\psi\rangle \ \forall \mathcal{M} \in \mathcal{U}\}. \tag{4}$$

Let G be the group constructed by the generators of spin-flip plaquette operators, i.e., X_p^C. The cardinality of the group is then $|G|=2^{|P|-2}$, where $|P|$ stands for the total number of plaquettes. Note that all plaquettes are not independent since the product of all plaquettes with the same color represents the same action in the group, namely, $\Pi_R X_p^C = \Pi_B X_p^C = \Pi_G X_p^C = X^{\otimes|V|}$, where $|V|$ stands for the number of all vertices. By starting from an initial vacuum state, say $|0\rangle^{\otimes|V|}$, where $Z|0\rangle=|0\rangle$, one can construct a state vector in the Hilbert space that is stabilized by the group elements. This state vector is a superposition of all elements of the stabilizer group with equal weights. From the previous arguments, it is convenient to denote it by $|0000\rangle$, which has the following form:

$$|0000\rangle = |G|^{-1/2} \sum_{g \in G} g|0\rangle^{\otimes|V|}, \tag{5}$$

where the g is an element of the stabilizing group, i.e., $g = \otimes_{p \in P} X_p^{r_p}$, where $r_p=0(1)$ corresponds to the plaquette operator X_p appearing (not appearing) in the element group g. There are many elements of the Pauli group that commute with all the elements of the stabilizer group but are not actually in G, and it is defined as the centralizer of G in the Pauli group. Since elements of the Pauli group either commute or anticommute, the centralizer is actually equal to the normalizer of G in the Pauli group. Considering the noncontractible loops, the normalizer of the stabilizer group can be obtained by a product of the stabilizer group and a group of noncontractible loop operators. Let us denote it by $\bar{G}=\mathcal{A}\cdot G$, where the group $\mathcal{A}$ is generated by noncontractible loop operators, i.e.,

$$\mathcal{A} = \left\{ \prod_{\mu=1,C=B,R}^{\mu=2g} (S_\mu^{CX})^{r_{\mu c}}, \ r_{\mu c} = 0,1 \right\}. \tag{6}$$

So, the group $\bar{G}$ reads

$$\bar{G} = \left\{ \prod_{\mu=1,C=B,R}^{\mu=2g} (S_\mu^{CX})^{r_{\mu c}} G, \ r_{\mu c} = 0,1 \right\}. \tag{7}$$

Note that $G \subseteq \bar{G}$. The group $\bar{G}$ is the normalizer of G in the Pauli group, so the normal subgroup G divides the group $\bar{G}$ into 2^{4g} cosets. The cardinality of the group will be $|\bar{G}| = 2^{|P|+4g-2}$. Therefore the protected subspace $\mathcal{C}$ is spanned by 2^{4g} states, which correspond to different cosets. In fact, elements in $\bar{G}-G$ take one encoded state of the stabilized subspace to another encoded state without leaving the stabilized subspace. For the states of the stabilized subspace we have, by construction,

$$\mathcal{C} = \{|ijkl\rangle: \ |ijkl\rangle = X_1^i X_2^j X_3^k X_4^l |0000\rangle\}, \tag{8}$$

where X_1, X_2, X_3, X_4 are defined in Eq. (3) and $i,j,k,l=0,1$. These topological nontrivial string operators can take one state of the coding space to another one, and any error of this type will not be detectable. A generic state can be a superposition of different vectors of coding space as follows:

$$|\Psi\rangle = \sum_{i,j,k,l} a_{i,j,k,l} |ijkl\rangle, \quad \sum_{i,j,k,l} |a_{i,j,k,l}|^2 = 1. \tag{9}$$

B. Protected subspace as a ground-state subspace

From a practical point of view it is important to find a state of quantum many-body systems for the implementation of universal quantum computation. We can provide a construction in which the protected subspace may be the ground state of a local Hamiltonian [17]. The subspace $\mathcal{C}$ is the ground state of the following exactly solvable Hamiltonian, i.e.,

$$H = -\sum_{p \in P} X_p - \sum_{p \in P} Z_p. \tag{10}$$

The ground state of this Hamiltonian is 2^{4g}-fold degenerate and topologically protected from local errors. Different states of the ground-state subspace, is clear from Eq. (8), are obtained by the product of noncontractible colored strings. Each state is characterized by a set of topological numbers, which are the sum of all z_v modula 2 along noncontractible loops. For example, for a generic state $|ijkl\rangle$ in Eq. (8) the topological numbers are $\Sigma_{v \in I_1^B} z_v = i$, $\Sigma_{v \in I_2^B} z_v = j$, $\Sigma_{v \in I_1^R} z_v = k$, and $\Sigma_{v \in I_2^B} z_v = l$, where the summations are evaluated in mod 2, z_v stands for the z component of the Z-Pauli matrix of vertex v and I_μ^C identifies a set of vertices (qubits) on a closed noncontractible loop with homology μ and color C. An excited state will arise when any of the stabilizing conditions in Eq. (4) is violated. In the energy unit, which is defined by Hamiltonian Eq. (10), the first excited state will be separated from the ground state by a gap of value 2.

III. REDUCED DENSITY MATRIX AND VON NEUMANN ENTROPY

In this section we calculate the entanglement properties of the topological color codes. We consider a generic bipartition of the system into subsystems A and B. Let Σ_A and Σ_B be the number of plaquette operators acting solely on A and B, respectively, and let Σ_{AB} stand for the number of plaquette operators acting simultaneously on A and B, i.e., these are boundary operators. We focus on the entanglement entropy between two partitions A and B of the system. To this end, first the reduced density operator of the one subsystem is evaluated and then the entanglement entropy is measured. If the state of the system is in an equal superposition of the elements of group G, the reduced density matrix for a subsystem, say A, has the following form [10]:

$$\rho_A = \frac{d_B}{|G|} \sum_{g \in G/G_B, \tilde{\rho} \in G_A} g_A |0_A\rangle\langle_A 0| g_A \tilde{g}_A, \tag{11}$$

where G_A and G_B are subgroups of G, which act trivially on subsystems B and A, respectively, and d_A and d_B are their cardinality. So the von Neumann entropy is

$$S_A = \log_2 |G_{AB}|, \tag{12}$$

where $G_{AB}=\frac{G}{G_A G_B}$. It is a simple task to show that all states of the coding space have the same entanglement entropy. To show this, let $X(t)=X_1^i X_2^j X_3^k X_4^l$ in which $t=(i,j,k,l)$ is a binary vector. So, for a generic state in the coding space we have $|t\rangle=X(t)|0\rangle$. Moreover, the string operators $X(t)$ can be decomposed as $X(t)=X(t)_A \otimes X(t)_B$. Therefore we obtain

$$\begin{aligned}\rho_A(|t\rangle) &= \mathrm{Tr}_B(|t\rangle\langle t|) = \mathrm{Tr}_B(X(t)|0\rangle\langle 0|X(t)) \\ &= X(t)_A \,\mathrm{Tr}_B(|0\rangle\langle 0|) X(t)_A \\ &= X(t)_A \rho_A(|0\rangle) X(t)_A. \end{aligned} \tag{13}$$

This implies that, by using the replica $S_A(t)=\lim_{n\to 1}\partial_n \mathrm{Tr}[\rho_A^n]$, the entanglement entropy for a state $|t\rangle$ is $S_A(t)=S_A(0)$.

IV. ENTANGLEMENT OF TCC FOR VARIOUS BIPARTITIONS

In this section we design different spin configurations as subsystems and then evaluate their entanglement with its complementary.

A. One spin

As the first example we consider the entanglement between one spin and the remaining ones of the lattice. In this case there are no closed boundary operators acting exclusively on the spin, i.e., subsystem A. So the reduced density matrix ρ_A is diagonal as follows:

$$\rho_A = f^{-1} \sum_{g \in G/G_B} g_A |0_A\rangle\langle_A 0| g_A, \tag{14}$$

where $f=|G/G_B|$ is the number of operators that act freely on the subsystem A. As it is clear, there are three plaquette operators that act freely on one spin since every spin in the color code is shared by the three plaquettes [see Fig. 1]. This leads to $f=2^3=8$. Only half of the operators of the quotient group lead to flipping the spin, i.e., they will have a trivial effect unless three plaquettes act either individually or altogether. Therefore the reduced density matrix is

$$\rho_A = \frac{1}{2}(|1_A\rangle\langle_A 1| + |0_A\rangle\langle_A 0|). \tag{15}$$

Thus, in topological color code every spin is maximally entangled with other spins. For the surface code (Kitaev model) a single spin is also maximally entangled with other spins [10].

B. Two spins

We calculate the entanglement between two spins. For this case also there is not any closed boundary operator with a nontrivial effect on two spins, so the reduced density matrix reads

$$\rho_A = \frac{1}{4}(|11\rangle\langle 11| + |10\rangle\langle 10| + |01\rangle\langle 01| + |00\rangle\langle 00|). \tag{16}$$

The entanglement between two spins, which is measured by the concurrence [18], vanishes. While each spin is maximally entangled with others, two spins are not entangled, which is a manifestation of the fact that the topological color code is genuinely multipartite entangled like the surface codes.

C. Colored spin chain

In this case we aim to know how much a closed colored spin chain winding the torus nontrivially, say blue or red in Fig. 1, is entangled with the rest of the lattice. For the sake of clarity and without loss of generality we consider a hexagonal lattice with $|P|=3k\times 4k$ plaquettes, where k is an integer number as $1,2,3\ldots$, for example, in Fig. 1, $k=2$. This choice makes the color code more symmetric. So, the number of plaquettes with a specific color, say red, is $(2k)^2$, and the number of spins that the colored chain contains is $4k$. Let the system be in the $|0000\rangle$. For this state there is not any closed boundary that exclusively acts on the chain. Therefore the reduced density matrix is diagonal and the number of plaquette operators that act independently on the subsystem B is

$$\Sigma_B = (|P|-2) - (3\times 2k) + (2k+1), \tag{17}$$

where the third term is the number of constraints on the plaquette operators acting on the spin chain. In fact, these are collective operators, i.e., products of boundary plaquette operators between A and B, which act solely on B. With these remarks in hand, the entanglement entropy becomes

$$S_A = \log_2 \frac{|G|}{d_B} = 4k-1. \tag{18}$$

It is instructive to compare the obtained entanglement entropy in Eq. (18) with the entanglement of the spin chain in Kitaev's model. For the latter case when the model is defined on the square lattice on a compact surface, i.e., torus, there exists a rather similar scaling with the number of qubits living in the chain [10].

In both cases the entanglement entropy in Eq. (18) can be understood from the fact that only configurations with an even number of spin flips of the chain are allowed in the ground-state structure. Plaquettes that are free to act on the spin chain are only able to flip an even number of spins of the chain. The same arguments can be applied for the other ground states $|ijkl\rangle$, where for all of them the entanglement entropy is given by Eq. (18). By inspection of the other ground states we see that there are $2^3=8$ states in which an even number of spins in the spin chain have been flipped. These states are

$$|0000\rangle,\quad X_1|0000\rangle,\quad X_3|0000\rangle,\quad X_4|0000\rangle,\quad X_1X_3|0000\rangle,$$

$$X_1X_4|0000\rangle,\quad X_3X_4|0000\rangle,\quad X_1X_3X_4|0000\rangle. \tag{19}$$

Besides, there are $2^3=8$ states with an odd number of spin flipped for the spin chain, which have been listed below.

$$X_2|0000\rangle,\quad X_2X_1|0000\rangle,\quad X_2X_3|0000\rangle,$$

$$X_2X_4|0000\rangle,\quad X_2X_1X_3|0000\rangle,\quad X_2X_1X_4|0000\rangle,$$

$$X_2X_3X_4|0000\rangle, \quad X_2X_1X_3X_4|0000\rangle. \tag{20}$$

Now we consider a generic state and calculate the entanglement entropy between the colored spin chain and the rest of the lattice. The density matrix $\rho=|\Psi\rangle\langle\Psi|$ is

$$\rho = \sum_{ijkl,mnpq} a_{ijkl}\bar{a}_{mnpq}X_1^iX_2^jX_3^kX_4^l\rho_0X_1^mX_2^nX_3^pX_4^q. \tag{21}$$

With the explanations we made above, the eigenvalues of the reduced density matrix ρ_A for the even number of spin flipped is as follows:

$$\frac{d_B}{|G|}(|a_{0000}|^2 + |a_{1000}|^2 + |a_{0010}|^2 + |a_{0001}|^2 + |a_{1010}|^2 + |a_{1001}|^2 + |a_{0011}|^2 + |a_{1011}|^2) = \frac{d_B}{|G|}\alpha, \tag{22}$$

where $\frac{|G|}{d_B}=2^{4k-1}$. Note that the number of these eigenvalues is 2^{4k-1}. Through the similar arguments we see that the eigenvalues of the reduced density matrix of the spin chain with an odd number of spin flipped is $\frac{d_B}{|G|}(1-\alpha)$ and the number of these eigenvalues is 2^{4k-1}. So, we can calculate the entanglement entropy as follows:

$$\begin{aligned} S_A &= -\sum_{i=1}^{2^{4k}} \lambda_i \log_2 \lambda_i \\ &= -2^{4k-1}\frac{d_B}{|G|}\alpha \log_2 \frac{d_B}{|G|}\alpha \\ &\quad - 2^{4k-1}\frac{d_B}{|G|}(1-\alpha)\log_2\left(\frac{d_B}{|G|}(1-\alpha)\right) \\ &= 4k - 1 + H(\alpha), \end{aligned} \tag{23}$$

where $H(x)=-x\log_2 x-(1-x)\log_2(1-x)$.

What about the entanglement of an open string? The open strings in the color code stand for the errors and map the coding space into an orthogonal one. These open strings anticommute with plaquette operators that share in an odd number of vertices. For an open string that contains k' qubits the entanglement entropy is $S_A=\log_2 \frac{|G|}{d_Bd_A}=k'$, i.e., an open string will be maximally entangled with the rest of the system.

D. Red strings crossing

As another bipartition we select all spins on the two red strings with different homologies, say X_1 and X_4 in Fig. 1, which have $2\times 4k=8k$ spins. Let the system be in the $|0000\rangle$ state. There is not any closed boundary operator acting solely on A. Considering the total number of independent plaquette operators acting solely on subsystem B, the entanglement entropy then reads

$$S_A = 8k - 1. \tag{24}$$

Again we see that there are only configurations with an even number of spins flipped in the construction of the state $|0000\rangle$. For a generic state as in Eq. (21) where we can realize all states with either an even or odd number of spin flips, the entanglement entropy will be

$$S_A = 8k - 1 + H(\alpha). \tag{25}$$

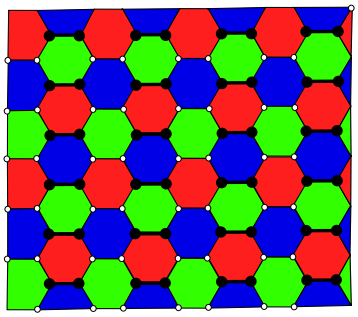

FIG. 2. (Color online) A set of vertical spin ladders (black solid circles) on 2-colex as a subsystem for calculating entanglement entropy.

E. Red and blue strings crossing

By this partition we mean the spins on the X_1 and X_2 strings in Fig. 1. The subsystem A contains $8k-1$ spins and again there is no closed boundary acting on it. Enumerating the independent plaquette operators acting on the subsystem B, the entanglement entropy is

$$S_A = 8k - 3. \tag{26}$$

F. Two parallel spin chains

Two parallel spin chains, say red and blue (X_1 and X_3) in Fig. 1, or equivalently, a green string, contain $2\times 4k=8k$ spins and again there is not any closed string acting on it nontrivially. $8k$ plaquettes act freely on subsystem A, but there are some constraints on them that arise from the product of plaquettes, which leave the subsystem A invariant and makes a collective operator, which acts solely on B. The product of blue and green plaquettes of those plaquettes that are free to act on A will produce a red string leaving A invariant. The same product holds for the red and green plaquettes. So the entanglement entropy reads

$$S_A = 8k - 2. \tag{27}$$

Indeed this is entanglement entropy for a green string. However, the number of spins it contains is twice over the strings we discussed in Sec. IV.

G. Spin ladder

A set of vertical spin ladders has been shown in Fig. 2. In this section only one of them has been considered as subsystem A. Let the system be in the state $|0000\rangle$. In this case the subsystem A contains $2\times 3k$ spins, and the total number of independent plaquettes acting on subsystem B is $(|P|-2)-3\times 3k+3k$. Since there are not any closed strings acting solely on A, the entanglement entropy reads

$$S_A = 6k. \tag{28}$$

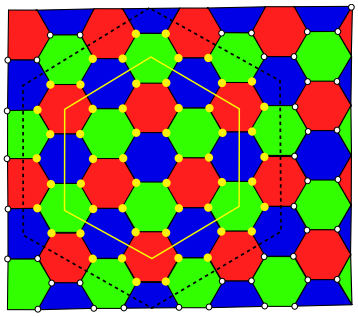

FIG. 3. (Color online) A manifestation of an hexagonal disk as a subsystem. A set of plaquettes is chosen in such a way that forms a large hexagon (the yellow line), and all large yellow (light) spins are in the subsystem. The dashed black line depicts the set of plaquettes acting simultaneously on both subsystems.

So, it is clear that this spin ladder has a maximum entanglement with the rest of the system and its state has the maximum mixing, namely,

$$\rho_A = 2^{-6k}\mathbf{I}_{6k\times 6k}. \tag{29}$$

H. Vertical spin ladders

Now we consider all vertical spin ladders as has been depicted in Fig. 2 and again we suppose the system is in the state $|0000\rangle$. There is not any plaquette operator that acts solely on subsystem A. However, there are several specific products of plaquette operators producing closed strings, which act solely on A. For example, the product of plaquettes that are in a vertical column will produce a closed string acting on one of the subsystems. Both subsystems A and B are symmetric with respect to each other. So, the number of closed strings that act only on A and B will be $d_A=d_B=2^{2k}$. Finally, the entanglement entropy reads

$$S_A = 12k^2 - 4k - 2. \tag{30}$$

I. Hexagonal disk

In this case we adapt a situation in which a set of plaquettes intuitively forms a hexagon as shown in Fig. 3. In this figure the dashed hexagon demonstrates a set of plaquettes lying between two subsystems. We suppose that the number of plaquettes crossed by the one edge of the hexagon be n. Now we can enumerate the number of plaquettes that act on A in terms of n, i.e., $\Sigma_A=3n(n-1)+1$. The total number of spins of the subsystem A is $6n^2$. There are $\Sigma_{AB}=6n$ plaquettes that act between A and B. Let the system be in the state $|0000\rangle$. With these realizations of the subsystems and since $|P|=\Sigma_A+\Sigma_B+\Sigma_{AB}$, we can turn on to calculate the entanglement entropy between two subsystems as follows:

$$S_A = \log_2 2^{\Sigma_{AB}-2} = \Sigma_{AB} - 2 = 6n - 2. \tag{31}$$

We can relate this entropy to the perimeter of the subsystem A by choosing the height of a plaquette as a unit. The perimeter of A is $\partial A=6n$ and the entropy will then be

$$S_A = \partial A - 2. \tag{32}$$

Generally, for an irregular lattice the entropy for a convex shape will be $S_A=\kappa\partial A-\gamma$ where the coefficient κ is a nonuniversal constant depending on the shape of the region, while the constant $\gamma=2$ will be universal and has a topological nature. So, we see that the entanglement entropy for the topological color code scales with the boundary of the subsystem, which is a manifestation of the so-called *area law* [11,19,20].

The latter relation we obtained for the entanglement entropy is consistent with the derivation of Kitaev *et al.* [12] and Levin *et al.* [13] where they proposed that for a massive topological phase there is a topological subleading term for the entanglement entropy that is related to the quantum dimension of the Abelian quasiparticles. The total quantum dimension for the topological color code will be

$$\gamma = \log_2 \mathcal{D}, \quad \mathcal{D} = 4. \tag{33}$$

The quantity $\mathcal{D}^2$ is the number of topological superselection sectors of Abelian anyons. For Kitaev's toric code there are only four such sectors leading to $\gamma=\log_2 2$. So the total quantum dimension in the topological color code is bigger than the toric code. The Abelian phase of the toric code is characterized via appearing in a global phase for the wave function of the system by winding an electric (magnetic) excitation around a magnetic (electric) excitation [12]. In the case of color code the excitations are colored and they appear as end points of open colored strings of a shrunk lattice [16]. Winding a colored X-type excitation around the Z-type one with a different color gives an overall factor $(-)$ for the wave function of the model, i.e., the phase is Abelian. Therefore the contribution of the color to the excitations makes the Abelian phase of the color code richer than the toric code with a bigger quantum dimension.

Now let the system be in a generic state such as Eq. (21). The reduced density matrix then reads

$$\rho_A = \sum_{ijkl,mnpq} a_{ijkl}\bar{a}_{mnpq}\,\mathrm{Tr}_B(X_1^iX_2^jX_3^kX_4^l\rho_0X_1^mX_2^nX_3^pX_4^q). \tag{34}$$

Some remarks are in order. For two different nontrivial closed string operators but with the same homology and color, say X and X', they will have the same support and are related via a trivial closed string $g\in G$, i.e., $X'=gX$. Since $[g,X]=0$, two strings will have the same effect on the ρ_0, i.e., $X'\rho_0=gX\rho_0=X\rho_0$. We can exploit this property of string operators in order to choose the strings appearing in Eq. (34) in which they do not cross subsystem A. Indeed the strings X_i act only on the subsystem B, i.e., $X_{iA}=\mathbf{I}_A$. This leads to $\mathrm{Tr}_B(X_i\rho_0X_i)=\mathrm{Tr}_B(\rho_0)$ for $i=1,2,3,4$ and $\mathrm{Tr}_B(X_1^iX_2^jX_3^kX_4^l\rho_0X_1^iX_2^jX_3^kX_4^l)=\mathrm{Tr}_B(\rho_0)$ for $i,j,k,l=0,1$. Other cases will be zero. To clarify this, let us for example, consider the simple case $\mathrm{Tr}_B(X_1\rho_0)$ where we have

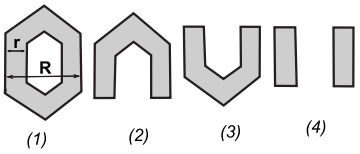

FIG. 4. Different bipartitions of the lattice in order to drop the bulk and boundary effect through the definition of topological entanglement entropy.

$$\mathrm{Tr}_B(X_1\rho_0) = \sum_{g,g'\in G} g_A|0_A\rangle\langle_A 0|g'_A \times \sum_{g''_B} \langle_B 0|g''_B X_4 g_B|0_B\rangle\langle_B 0|g'_B g''_B|0_B\rangle = \sum_{g,g'\in G} g_A|0_A\rangle\langle_A 0|g'_A\langle_B 0|g'_B X_B g_B|0_B\rangle. \quad (35)$$

On the other hand, from the group property $g'=g\tilde{g}$ the above expression becomes

$$\mathrm{Tr}_B(X_1\rho_0) = \sum_{g,\tilde{g}\in G} g_A|0_A\rangle\langle_A 0|g_A\tilde{g}_A\langle_B 0|\tilde{g}_B X_B|0_B\rangle, \quad (36)$$

which implies that $\tilde{g}_B=X_B$. Otherwise the above expression will become zero. The fact $\tilde{g}=\tilde{g}_A\otimes\tilde{g}_B\in G$ explicitly implies that the operator $\tilde{g}_A$ must be a noncontractile string, which is impossible since it must act solely on A. So we will leave with $\mathrm{Tr}_B(X_1\rho_0)=0$. The same arguments may also apply for other cases. Finally, the entanglement for a generic state of the system and a convex region will become

$$\rho_A = \mathrm{Tr}_B(\rho_0), \quad S_A = \partial A - 2. \quad (37)$$

J. Topological entanglement entropy

As we can see from Eq. (32), in the entanglement entropy of a region there exists a subleading term that is universal and independent of the shape of region. This is a characteristic signature of topological order, which has been found on the subleading term of the entanglement entropy. To be more precise on the topological character of the subleading term, we can construct a set of bipartitions in which the boundary contribution is dropped and the remaining term is stemmed from the topological nature of the code and inspires the topological order. To drop the bulk and boundary degrees of freedom we consider a set of partitions that have been shown in Fig. 4. Topological entanglement entropy then arises from the following combination of entanglement entropy:

$$S_{topo} = \lim_{R,r\to\infty}(-S_{1A}+S_{2A}+S_{3A}-S_{4A}). \quad (38)$$

For each bipartition one can use the entanglement entropy as before, namely, $S_G=\log_2(|G|)-\log_2(d_A d_B)$. So far the cardinalities d_A and d_B were determined by the number of plaquette operators acting solely on A and B, respectively, i.e., $d_A=2^{\Sigma_A}$ and $d_B=2^{\Sigma_B}$, where Σ_B and Σ_B stand for the number of plaquette operators acting only on A and B, respectively. However, for the calculation of the S_{topo} we should take into account other closed strings in addition to the above closed strings acting on subsystems. For the case in which each partition is a single connected region, for example, bipartitions (2) and (3) in Fig. 4, the previous arguments work, but for disjoint regions such as (1) and (4) in Fig. 4 we should extend the above result. As an example a simple case has been shown in Fig. 5 where we have supposed the subsystem A is composed of two disjoint regions (two dashed rectangles, which we label as A_1 and A_2), while the subsystem B is a single connected one. By inspection we see that the product of two sets of plaquettes, say the blue and green ones, which act on A_1, and the blue and green ones acting simultaneously on A_1 and B, result in a red string that acts only on B. The same scenario can be applied for other choices of the plaquettes, e.g., red and green or red and blue plaquettes, which yield blue and green strings leaving the subsystem A_1. However, as we pointed out before, one of them will be immaterial since there is an interplay between homology and color.

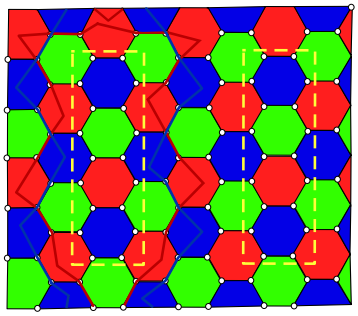

FIG. 5. (Color online) One of the subsystems, say A, composed of two disjoint regions that introduce some nontrivial colored closed strings acting solely on B. The closed blue and red strings have been shown only for one region of subsystem A.

The main point is that it is not possible to produce these colored closed strings that act only on B from the product of some plaquettes of region B. The same thing will be held for another disjoint region of A, say A_2. So, we have a collection of closed strings with a nontrivial effect on B and we must take them into account in the calculation of d_B. But, a remark is in order and that if, for example, we combine two red strings, the resultant is not a new closed string because we can produce these two red strings from the product of the blue and green plaquettes of region B. Therefore for the case shown in Fig. 5 there are only two independent closed strings of this type with a nontrivial effect on B. With these remarks, now the cardinalities d_A and d_B are

$$d_A = 2^{\Sigma_A}, \quad d_B = 2^{\Sigma_B+4-2}. \quad (39)$$

We can generalize the above results for the case that each subsystem is composed of several disconnected regions. Let the partitions A and B be composed of m_A and m_B disjoint regions, respectively. So, the cardinalities will be

$$d_A = 2^{\Sigma_A+2m_B-2}, \quad d_B = 2^{\Sigma_B+2m_A-2}. \quad (40)$$

Now we move on in order to calculate the topological entanglement entropy defined in Eq. (38). For the partitions shown in Fig. 4 we have

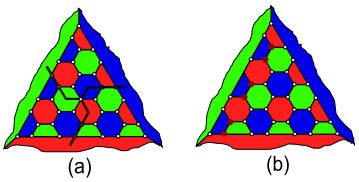

FIG. 6. (Color online) A class of color code on the plane. It includes borders, each of one color. It encodes one qubits and can be produced from a 2-colex without a border by removing a couple of plaquettes. To each border only strings with the same color of border can have end points. (a) three-string net commutes with all plaquette operators. Such a string net and its deformation makes the encoded Pauli operators acting on the encoded qubit. (b) A manifestation of colored string as a bipartition. It stands for an error.

$$m_{1B} = m_{4A} = 2,$$

$$m_{1A} = m_{2A} = m_{2B} = m_{3A} = m_{3B} = m_{4B} = 1, \tag{41}$$

$$\Sigma_{1A} + \Sigma_{4A} = \Sigma_{2A} + \Sigma_{3A}. \tag{42}$$

Finally, the topological entanglement entropy reads as follows:

$$S_{topo} = -4. \tag{43}$$

Topological entanglement entropy depends only on the topology of the regions with no matter to their geometries [12]. This derivation for the topological entanglement entropy of color codes is consistent with the subleading term of scaling of the entropy. The topological entanglement entropy is related to the subleading term of the entanglement entropy, i.e., $S_{topo}=-2\gamma$ [12]. This leads to $\gamma=2$, which has also been derived in Eq. (32).

V. ENTANGLEMENT PROPERTIES OF PLANAR COLOR CODES

An important class of topological stabilizer codes in practice is planar codes, which are topological codes that can be embedded in a piece of planar surface. These planar codes are very interesting for topological quantum memory and quantum computations [9,15]. A planar color code will be obtained from a 2-colex without a border when a couple of plaquettes are removed from the code. For example, when a plaquette, say green, is removed, only green strings can have an end point on the removed plaquette, not the blue and red strings. The same scenario holds for other plaquettes. By this construction we will end with a 2-colex that has three borders, each of one color. To each border only strings can have end points which have the same color of that border. The most important class of such a planar color code is the triangular code that has been shown in Fig. 6. The essential property of such a code is determined via realizing a three-string operator and its deformation. We denote them by T^X and T^Z so that $\{T^X, T^Z\}=0$ since they cross each other once at strings with different colors. This latter anticommutation relation can also be invoked by considering all qubits, which makes the triangular color code very interesting for full implementation of the Clifford group without a need for selective addressing [15]. Instead of giving such fruitful properties, we are interested in the entanglement properties of the triangular code.

To have a concrete discussion, we consider a triangular lattice that contains hexagons like what has been shown in Fig. 6. The total number of plaquettes and vertices are $|P| = \frac{3}{2}k(k+1)$ and $|V|=3k(k+1)+1$, respectively, where k is an integer number. The plaquette operators like those defined in Eq. (1) have been used in order to define a stabilizer subspace for this code. A main point about the planar code is that there are no constraints on the action of plaquette operators, i.e., they are independent. For example, if we produce all red and green plaquette operators, the resulting operator will not be the same with the product of red and blue plaquette operators, a property that was absent for the color code on the compact surface. However, the product of distinct plaquettes is in the stabilizer group. The coding space is spanned with the states that are fixed points of all plaquette operators. With the above identifications for the number of plaquettes and vertices, the dimension of the coding space will be $\Lambda=\frac{2^{|V|}}{2^{|P|}2^{|P|}}=2$. This implies that the triangular code encodes a single qubit. Two states are completely determined by the elements of the stabilizer group and three-string operator. Note that here the three-string operator plays a role like nontrivial closed strings in the color code on the torus. For triangular code the 3-string is nontrivial, i.e. it commutes with all plaquette operators and is not a product of some plaquettes. So the stabilized states will be

$$|0\rangle = |G|^{-1/2} \sum_{g \in G} g|0\rangle^{\otimes |V|}, \quad |1\rangle = T^X|0\rangle. \tag{44}$$

A generic state can be in a superposition of the above states such as $|\psi\rangle=\Sigma_{i=0}^{1}a_i|i\rangle$ where $\Sigma_{i=0}^{1}|a_i|^2=1$. The reduced density matrix in Eq. (11) gives what we need to evaluate the entanglement entropy. Again we make different bipartitions and calculate the entanglement entropy.

Let the system be in the state $|0\rangle$. A single qubit is maximally entangled with the rest of the system while two qubits are not entangled implying that the triangular code is also a multipartite entangled structure. As another bipartition we consider a colored spin chain such as the red chain in Fig. 6(b). This string contains $2k$ qubits and anticommutes with plaquettes, which the string has an endpoint on them, i.e., they share an odd number of qubits, thus its action on the coding space amounts to an error or on the other hand, to the appearance of excitations above the ground state if we adopt the coding space as a ground state of a local Hamiltonian as in Eq. (10). However, such a string has maximal entanglement $S_A=2k$ with other qubits of the lattice. This means that all configurations of the spin chain are allowed in the state $|0\rangle$ of the code, a feature that is similar to the entanglement of an open string in the topological color code on the torus [see Sec. IV C].

Taking into account the qubits living on the three-string net as subsystem A leads to the occurrence of configurations of subsystem A with only an even number of spins flipped in the state $|0\rangle$. For this string net as shown in Fig. 6(a) the number of qubits of the string is $2k+1$, and the entanglement

entropy then will become $S_A=2k$. By inspection we see that the plaquette operators flip only an even number of qubits of the string net. Now let the system be in a generic state such as $|\psi\rangle$. All possible configurations of the string net are allowed since all of them can be realized by applying some three-string operators T^X. There are 2^{2k} configurations with an even number of spins flipped and 2^{2k} configurations with an odd number of spins flipped. The states $|0\rangle$ and $|1\rangle$ include even and odd configurations, respectively. Therefore the entanglement entropy for a generic state will be $S_A=2k+H(\alpha)$, where $\alpha=|a_0|^2$.

What about the topological entanglement entropy of planar color codes? In order to answer this question we obtain a set of bipartitions such as in Fig. 4 in a large triangular code. Let Σ_A and Σ_B stand for the number of plaquette operators acting only on A and B, respectively, and Σ_{AB} stands for the number of plaquette operators acting simultaneously on A and B. All plaquette operators are independent. To make things simpler, let us consider a simple case where the subsystem A is a single convex connected region. The cardinality of the subgroup G_A is 2^{Σ_A}. However, there are two nontrivial closed strings acting on subsystem B, which is impossible to provide them by the product of some plaquettes of B. In fact these two independent strings result from the product of some plaquettes, say red and green, which are free to act on A. So the cardinality of the subgroup B reads 2^{Σ_B+2}. Thus for the entanglement entropy we obtain $S_A=\Sigma_{AB}-2$.

In order to calculate the topological entanglement entropy, first the entanglement entropy is calculated for different bipartitions and then the expression in Eq. (38) gives the topological entropy. Because of the boundaries in the planar codes, for a disconnected region like (1) or (4) in Fig. 4 the constraint we imposed in Eq. (40) is no longer true. For the bipartition (1) in Fig. 4 the cardinalities of subgroups G_A and G_B will be $d_A=2^{\Sigma_{1A}+2}$ and $d_B=2^{\Sigma_{1B}+2}$, respectively. However, for the bipartitions (4) in Fig. 4 the cardinalities will be $d_A=2^{\Sigma_{4A}}$ and $d_B=2^{\Sigma_{4B}+4}$, respectively. Thus the topological entanglement entropy becomes $S^t_{topo}=-4$. Although the closed string structures of bipartitions in the triangular code due to the boundary effects differ from the color code on the torus, the topological entanglement entropy is the same for both structures that are related to the fact that both structures have the same symmetry.

VI. CONCLUSIONS

In this paper we calculated the entanglement properties of topological color codes (TCC) defined on a two-dimensional lattice. The entanglement entropy was measured by the von Neumann entropy. We considered two structures of TCC, either defined on the compact or planar surface. The coding space of TCC is spanned by a set of states in which are the fixed points of a set of commuting Pauli operators, i.e., they are common eigenvectors of all elements of the stabilizer group with an eigenvalue +1. In fact this set stabilizes the coding space. The stabilizer group is generated from plaquette operators. The product of different plaquette operators produces colored strings, which in fact are the closed boundary of several plaquettes. However, there exist some independent nontrivial strings winding the handles of the manifold where the model is defined on. These nontrivial strings commute with all plaquette operators but are not actually in the stabilizer group. These nontrivial strings make remarkable properties of the color code more pronounced.

The coding space of lattice embedded in a manifold with genus g is spanned by 4^{2g} states. This coding space can be adopted in which be a ground state subspace of a local Hamiltonian. The degeneracy of the ground-state subspace depends on the genus of the manifold, which is a feature of topological order. Different states of the ground-state subspace can be constructed by means of spin-flipped elements of the stabilizer group and nontrivial closed loops. In order to calculate the entanglement properties of the TCC, the reduced density matrix of a subsystem is obtained by integrating out the remaining degrees of freedom. We did this by using the group properties of the stabilizer group.

For both structures of color code on compact and planar surfaces while a single qubit is maximally entangled with others, two qubits are no longer entangled. This finding manifests that the color code is a genuinely multipartite entangled structure. We also considered other bipartitions such as spin chains, spin ladders with various colors, and homologies. For all bipartitions we found the entanglement entropy depends on the degrees of freedom living on the boundary of two subsystems. However, in the entanglement entropy of a convex region, there is a subleading term that is ascribed to the topological properties of region, not the geometry, a feature that has also arisen in a massive topological theory [12]. The fact that the entanglement entropy for a region of lattice scales with its boundary is a feature of *area law* is also of great interest in other branches of physics such as black holes [21].

We exploited the scaling of the entropy to construct a set of bipartitions in order to calculate the topological entanglement entropy of color codes. We find that it is twice over the topological entropy in the topological toric code. The nonvanishing value for topological entanglement entropy and dependency of degeneracy on the genus of the surface demonstrate remarkable features on the fact that topological color code is fabric to show topological order. For the toric code model the total quantum dimension of excitation is 4, which stands for different superselection sectors of its anyonic excitations. The total quantum dimension of color code is 16 inspiring that the topological color codes may carry richer anyonic quasiparticles. They may be colored and their braiding will have a nontrivial effect on the wave function of the system. Indeed braiding of a colored quasiparticle around the other one with a different color will give rise to a global phase for the wave function, i.e., they are Abelian excitations. A triangular color code with a remarkable application for entanglement distillation is also a highly entangled code. Although the colored strings employed in the 2-colex in the compact surface are not relevant in the triangular code, the notion of string net gives some essential properties to the triangular code. In the state of the triangular code all configurations of a colored string, say a red one in Fig. 6(b), are allowed, i.e., it has maximal entanglement with the rest of the system. However, for a string net only the configurations

with an even number of spins flipped are allowed. Entanglement entropy scales with a boundary of the region and includes a topological term. This topological term yields a nonvanishing topological entanglement entropy, which is the same as what we obtained for the color codes on the torus. Similar entanglement properties of color codes defined on the compact and planar surface are not a matter of chance because both structures carry the same symmetry.

ACKNOWLEDGMENTS

I would like to thank A. Langari for fruitful discussions and comments. I would also like to acknowledge M. A. Martin-Delgado for his useful comments. This work was supported in part by the Center of Excellence in Complex Systems and Condensed Matter (www.cscm.ir).

[1] S. Oh and J. Kim, Phys. Rev. B **71**, 144523 (2005).
[2] V. Vedral, New J. Phys. **6**, 102 (2004).
[3] X. G. Wen, Phys. Lett. A **300**, 175 (2002).
[4] L. Amico, R. Fazio, A. Osterloh, and V. Vedral, Rev. Mod. Phys. **80**, 517 (2008).
[5] N. Goldenfeld, *Lectures on Phase Transitions and the Renormalization Group* (Westview Press, 1992).
[6] X. G. Wen and Q. Niu, Phys. Rev. B **41**, 9377 (1990); X. G. Wen, Phys. Rev. Lett. **90**, 016803 (2003).
[7] A. Y. Kitaev, Ann. Phys. (N.Y.) **303**, 2 (2003).
[8] D. Gottesman, Phys. Rev. A **54**, 1862 (1996).
[9] E. Dennis, A. Kitaev, A. Landahl, and J. Preskill, J. Math. Phys. **43**, 4452 (2002).
[10] A. Hamma, R. Ionicioiu, and P. Zanardi, Phys. Rev. A **71**, 022315 (2005); A. Hamma, R. Ionicioiu, and P. Zanardi, Phys. Lett. A **337**, 22 (2005).
[11] S. Ryu and T. Takayanagi, J. High Energy Phys. (2006) 045.
[12] A. Kitaev and J. Preskill, Phys. Rev. Lett. **96**, 110404 (2006).
[13] M. Levin and X. G. Wen, Phys. Rev. Lett. **96**, 110405 (2006).
[14] H. Bombin and M. A. Martin-Delgado, Phys. Rev. Lett. **97**, 180501 (2006).
[15] H. Bombin and M. A. Martin-Delgado, Phys. Rev. A **76**, 012305 (2007).
[16] H. Bombin and M. A. Martin-Delgado, Phys. Rev. B **75**, 075103 (2007).
[17] R. Raussendorf, S. Bravyi, and J. Harrington, Phys. Rev. A **71**, 062313 (2005).
[18] W. K. Wootters, Phys. Rev. Lett. **80**, 2245 (1998).
[19] M. B. Plenio, J. Eisert, J. Dreißig, and M. Cramer, Phys. Rev. Lett. **94**, 060503 (2005).
[20] R. Bousso, Rev. Mod. Phys. **74**, 825 (2002).
[21] S. Ryu and T. Takayanagi, Phys. Rev. Lett. **96**, 181602 (2006).